

Dual-mode Operation of the Finger-type Manipulator Based on Distributed Actuation Mechanism

Jong Ho Kim¹, Young June Shin², Sung-Hwan Kim³, In Gwon Jang¹

¹ KAIST, Daejeon, Republic of Korea, jonghokim@kaist.ac.kr; igjang@kaist.edu

² Agency for Defense Development, Daejeon, Republic of Korea, yjshin@add.re.kr

³ Samsung Electronics, Suwon, Republic of Korea, murphy99@kaist.ac.kr

1. Abstract

Using the distributed actuation mechanism recently developed, this paper proposes the dual-mode operation of a finger-type manipulator that can switch between the force and velocity modes in order to achieve either the maximum force or the maximum velocity with the limited actuation power. The mathematical equations are derived for the fingertip force and velocity. Then, optimization scheme determines the maximum force and velocity that a finger-type manipulator can achieve at the given fingertip position along the given task direction. The numerical examples clearly demonstrate the effectiveness of the proposed dual-mode operation, which can enhance the operational efficiency of a manipulator in terms of velocity and/or force.

2. Keywords: dual-mode operation, distributed actuation mechanism, finger-type manipulator, design optimization, structural redundancy.

3. Introduction

For several decades, versatile manipulation systems have been applied to various fields such as military, service, and clinics. However, the performances of the state-of-the-art systems are not satisfactory because the performance of an actuator itself appears to be saturated (or slowly improve). A variety of researches have been investigated in order to provide an alternative solution for the current actuators, including the development of a new actuator such as artificial muscle [1]-[2], the enhancement of motor efficiency [3]-[4], and a new mechanism design [5]-[6]. They partially contribute to performance enhancement, but much remains to be improved.

In particular, the severe limitations in installation space and supplying power are an immense challenge to overcome in wearable robots. Considering that the actuating mechanism of a manipulator affects its system performance, the authors recently proposed the distributed actuation mechanism [7] that can provide additional degrees of freedom in actuation. The experiments validated the improvement of fingertip force through changing the posture angle and slider positions of the distributed actuation mechanism. Due to the increased complexity, however, more systematic approach is necessary to thoroughly analyse the distributed actuation mechanism.

This paper proposes the dual-mode operation of the distributed actuation mechanism in order to enhance the usability and efficiency during operation. The force and velocity of a finger-type manipulator were first derived in terms of control parameters (i.e. one posture angle, three slider positions, and three thrusting parameters). Then, design optimization for maximizing fingertip force and velocity determined the force and velocity modes, respectively, of the finger-type manipulator. Furthermore, the force and velocity octagons were obtained in order to effectively represent the allowable force and velocity, respectively, along the eight task directions at the given fingertip position. Based on these quantitative information, the appropriate trajectory and corresponding actuation control can be determined for the given tasks. Thus, the dual-mode distributed actuation mechanism can provide more efficient operation.

4. Mathematical Derivation of Dual-mode Distributed Actuation Mechanism

In [7], the distributed actuation mechanism, which is a multi-linked mechanism with sliding actuation, was proposed in order to implement the spatially distributed actuation of muscles, as illustrated in Figure 1. It was proven that this mechanism can provide a range of fingertip forces through relocating the slider positions at the given fingertip position. The goal of this paper is to propose the dual-mode operation of the distributed actuation mechanism for more efficient operation through maximizing either fingertip force or velocity.

In this section, mathematical equations for fingertip force and velocity were derived with the notations as follows:

l_j : length of the link j

c_j : length of the connecting rod at the joint j

θ_j : joint angle at the joint j

h : slider hinge offset

x_j and x_{bj} : positions of the front and back sliders at the joint j , respectively

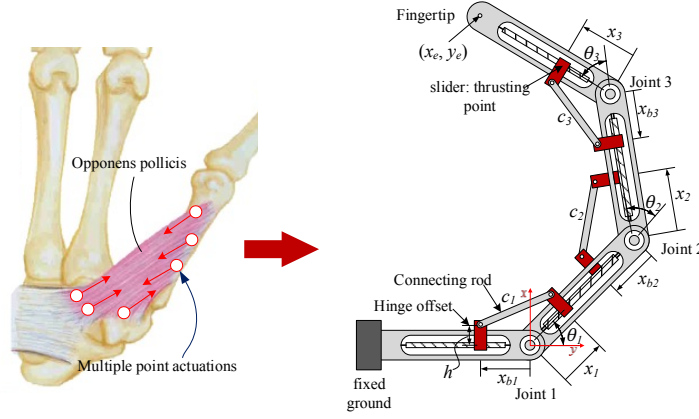


Figure 1: Concept of a distributed actuation mechanism for a robot finger using a sliding actuation [7]

4.1. Derivation of Fingertip Velocity

As illustrated in Figure 1, a robot finger with distributed actuation mechanism can be considered as a three-link planar manipulator, in which the fingertip at (x_e, y_e) has the generalized planar velocity, $\mathbf{v}_e = [x_e \ y_e \ \theta_e]^T$. At the fingertip position, θ_2 and θ_3 can be expressed in terms of θ_1 using the inverse kinematics. Figure 2 presents the trigonometric relationship of each joint as follows:

$$c_j^2 = x_j'^2 + x_{bj}'^2 + 2x_j'x_{bj}' \cos \theta_j \quad (1)$$

where $x_j' = x_j - h \tan(\theta_j/2)$ and $x_{bj}' = x_{bj} - h \tan(\theta_j/2)$. Through differentiating Eq. (1) with respect to time, the joint angular velocity was derived as follows:

$$\theta_j = \frac{\left(x_{bj} - h \tan \frac{\theta_j}{2}\right) \left(x_j \cos \theta_j + x_{bj}\right) + \left(x_j - h \tan \frac{\theta_j}{2}\right) \left(x_j + x_{bj} \cos \theta_j\right)}{\sin \theta_j \left(x_j - h \tan \frac{\theta_j}{2}\right) \left(x_{bj} - h \tan \frac{\theta_j}{2}\right) + \frac{1}{2} h \sec^2 \frac{\theta_j}{2} (1 + \cos \theta_j) \left\{ \left(x_j - h \tan \frac{\theta_j}{2}\right) + \left(x_{bj} - h \tan \frac{\theta_j}{2}\right) \right\}} \quad (2)$$

where $x_{bj} = \sqrt{c_j^2 - \left\{ \left(x_j - h \tan \frac{\theta_j}{2}\right) \sin \theta_j \right\}^2} - \left(x_j - h \tan \frac{\theta_j}{2}\right) \cos \theta_j + h \tan \frac{\theta_j}{2}$. Then, the fingertip velocity was determined through the differential kinematics as follows:

$$\mathbf{v}_e = \mathbf{J}(\boldsymbol{\theta})\boldsymbol{\theta} \quad (3)$$

where $\mathbf{J}(\boldsymbol{\theta})$ is a 3×3 Jacobian matrix.

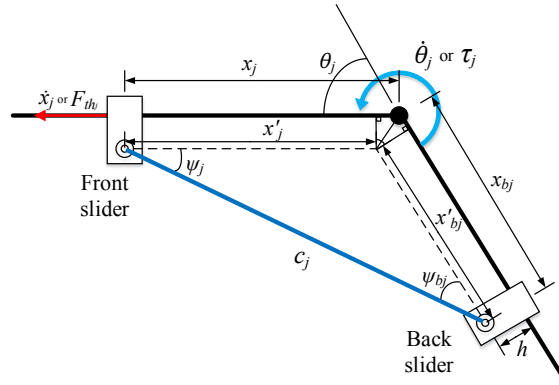


Figure 2: Schematic diagram of the joint j

4.2. Derivation of Fingertip Force

In order to derive the fingertip force of a kinematically redundant manipulator, the additional rotational degrees of freedom at the fingertip were provided as follows:

$$\mathbf{x}_e = [x_e \quad y_e \quad \theta_e]^T \text{ and } \mathbf{F}_e = [F_x \quad F_y \quad M_z]^T. \quad (4)$$

Through the procedure explained in [7], the joint torque was derived as follows:

$$\tau_j = F_{thj} \frac{x_j \tan \psi_j + h}{1 + \mu_j \tan \psi_j} \quad (5)$$

where $\psi_j = \cos^{-1} \left(c_j^2 + \left(x_j - h \tan \frac{\theta_j}{2} \right)^2 - \left(x_{bj} - h \tan \frac{\theta_j}{2} \right)^2 \right) / 2c_j \left(x_j - h \tan \frac{\theta_j}{2} \right)$; F_{thj} and μ_j are the thrusting force and the Coulomb friction coefficient at the joint j . Based on the static force equilibrium, the fingertip force was derived as follows:

$$\mathbf{F}_e = \mathbf{J}^{-T}(\boldsymbol{\theta}) \boldsymbol{\tau} \quad (6)$$

where $\mathbf{J}^{-T}(\boldsymbol{\theta})$ means a transposed matrix of the inverse Jacobian.

6. Numerical Simulation for Dual-mode Distributed Actuation Mechanism

6.1. Optimization for the maximum fingertip force and velocity

To determine the maximum fingertip force and velocity, optimization formulations were expressed as follows:

1) Force mode

$$\begin{aligned} \text{Maximize} \quad & F_{d_j}(\theta_1, x_i, F_{thi}) = \mathbf{F}_e \cdot \mathbf{d}_j \quad i = 1, 2, 3; j = 1, \dots, 8 \\ \text{subject to} \quad & \theta_1^{(l)} \leq \theta_1 \leq \theta_1^{(u)} \\ & x_i^{(l)} \leq x_i \leq x_i^{(u)} \quad i = 1, 2, 3 \\ & -F_{thi}^{(u)} \leq F_{thi} \leq F_{thi}^{(u)} \quad i = 1, 2, 3 \\ & M_z \cdot \theta_e \geq 0 \\ & F_x \cdot x_e + F_y \cdot y_e \geq 0 \end{aligned} \quad (7)$$

2) Velocity mode

$$\begin{aligned} \text{Maximize} \quad & v_{d_j}(\theta_1, \dot{x}_i, x_i) = \mathbf{v}_e \cdot \mathbf{d}_j \quad i = 1, 2, 3; j = 1, \dots, 8 \\ \text{subject to} \quad & \theta_1^{(l)} \leq \theta_1 \leq \theta_1^{(u)} \\ & \dot{x}_i^{(l)} \leq \dot{x}_i \leq \dot{x}_i^{(u)} \quad i = 1, 2, 3 \\ & -\dot{x}_i^{(u)} \leq \dot{x}_i \leq \dot{x}_i^{(u)} \quad i = 1, 2, 3 \\ & M_z \cdot \theta_e \geq 0 \\ & F_x \cdot x_e + F_y \cdot y_e \geq 0 \end{aligned} \quad (8)$$

where \mathbf{d}_j denotes a unit vector which forms a vertex of a regular octagon centered at the origin; F_{thi} and \dot{x}_i represent the thrusting force and velocity of a slider at the joint i , respectively. Design variables are one posture angle (θ_1), three slider positions (x_j), and three thrusting parameters (F_{thi} for the force mode or \dot{x}_i for the velocity mode). The lower and upper bounds for θ_1 were set to avoid the singular postures between 20° and 90° . The lower and upper bounds for x_i , \dot{x}_i , F_{thi} , and x_{bi} were also set considering the geometrical and physical limitations. Note that the lower bounds of thrusting force and velocity were set to be negative values of their upper bounds in order to represent movements in the opposite direction. Constraints for positive rotational and translational power at the fingertip were implemented to obtain physically meaningful results. Through the optimization formulated in Eqs. (7) and (8), the maximum fingertip force and velocity along the eight task directions ($\mathbf{d}_j, j=1, \dots, 8$) were determined. Design parameters used in optimization were listed in Table 1.

Table 1: Design parameters for the distributed actuation mechanism

	Joint 1	Joint 2	Joint 3
Link length [mm]	$l_1=114$	$l_2=114$	$l_3=109.6$
Connecting rod [mm]	$c_1=80$	$c_2=80$	$c_3=80$
Friction coefficient	$\mu_1=0$	$\mu_2=0$	$\mu_3=0$
Hinge offset [mm]	15.5		
Max. motor torque [gf·cm]	780		
Max. motor speed [rpm]	39		
Max. motor power [mW]	30.7		

Specifications for actuation were based on the electric motor, PGM12-1230E(3V), whose gear ratio is 1/256. Figure 3 depicts the workspace of a robot finger (grey area enclosed by black lines) and eight fingertip positions (red circles with their own numbers) to be analysed. The origin of the graph represents the base of a robot finger. In order to solve Eqs. (7) and (8), sequential quadratic programming method in MATLAB fmincon was used.

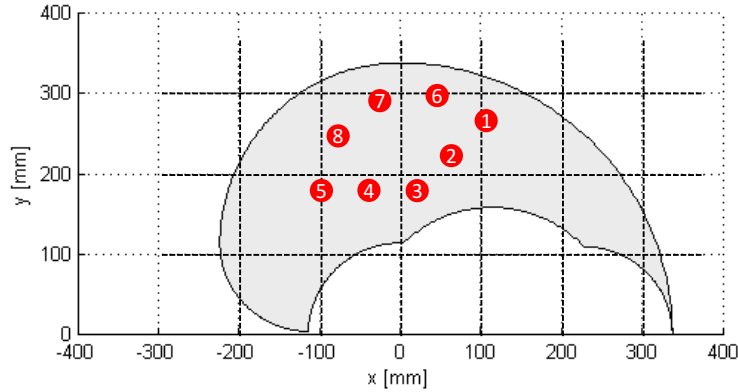


Figure 3: Target fingertip positions in workspace

6.2. Optimization results and discussion

To demonstrate the effectiveness of the proposed dual-mode operation, the maximum velocity and force were obtained. For Position 8 along the negative x direction, for example, the optimized posture angles and slider positions were illustrated as blue lines and green squares, respectively, for the force mode; red lines and orange squares for the velocity mode (Figure 4). Table 2 demonstrates that the difference of the control parameters between the force and velocity modes affects the performance at the same fingertip position.

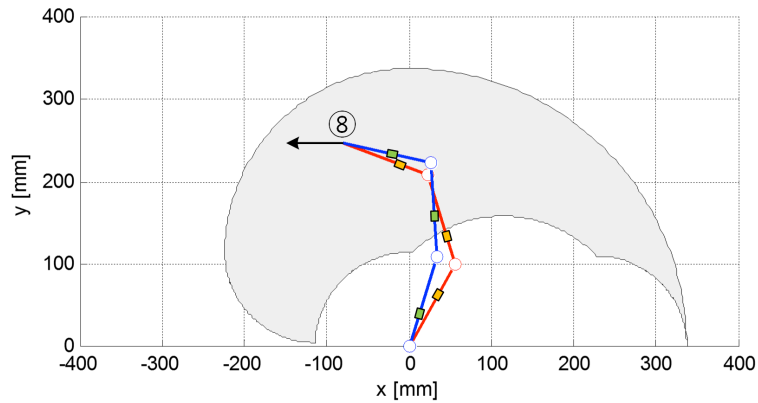


Figure 4: Optimized posture angle and slider positions for Position 8 (blue lines for the force mode and red lines for the velocity mode)

Table 2: Optimization results for Position 8 along the negative x direction

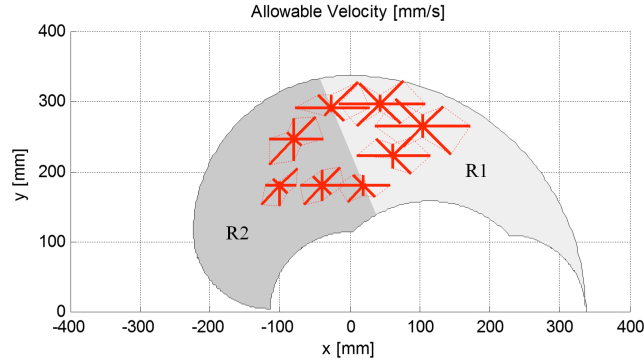
	θ_1 [°]	x_1 [mm]	x_2 [mm]	x_3 [mm]	Force	Velocity
Force mode	73.03	42.07	49.68	43.76	16.18 [N]	1.26 [mm/s]
Velocity mode	60.90	71.75	37.00	66.86	0.26 [N]	4.52 [mm/s]

As depicted in Figure 5, the velocity and force octagons (red-dotted lines and blue-dotted lines, respectively) represent the approximate, allowable values at the given fingertip position. Information on force and velocity octagons can be utilized in order to plan the optimal trajectory of a manipulator in the workspace. All the corresponding control parameters for operation can be obtained from the optimization. For example, suppose that a certain task starts at Position 1 and ends at Position 5. The task is also required to provide a fast motion in Region R1 and to generate a large force in Region R2. Then, the system performance during operation significantly depends on the trajectory as follows:

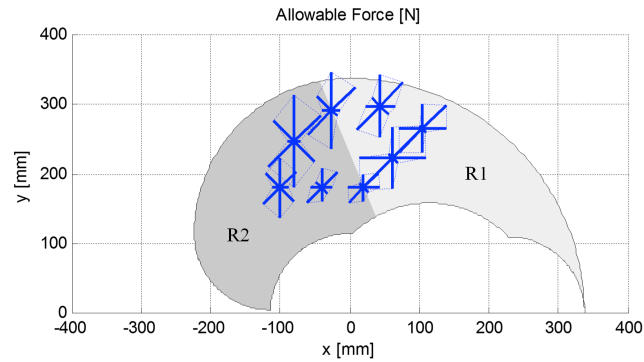
- 1) Path 1-6-7-8-5
Fast motion and large force are available in R1 and R2, respectively.
- 2) Path 1-2-3-4-5

Slower motion in R1 and smaller force in R2 are achieved although the maximum thrusting force and velocity of sliders are identical.

Table 3 indicates that the maximum value even at the same fingertip position significantly varies depending on the task direction (specifically, ranging from 2.61 to 8.22 for force or from 2.04 to 11.54 for velocity). Thus, more efficient operation will be possible for the given task if the trajectory and corresponding control parameters are appropriately determined.



(a) Velocity octagon



(b) Force octagon

Figure 5: Allowable velocity and force at various fingertip positions in workspace

Table 3: Summary of optimization results for dual-mode operation

	Point 1	Point 2	Point 3	Point 4
F_{max}/F_{min}	$F_{d6}/F_{d8}=8.22$	$F_{d6}/F_{d8}=7.56$	$F_{d6}/F_{d8}=3.28$	$F_{d6}/F_{d8}=2.61$
V_{max}/V_{min}	$V_{d5}/V_{d7}=4.11$	$V_{d5}/V_{d6}=11.54$	$V_{d5}/V_{d2}=9.51$	$V_{d6}/V_{d8}=2.04$
	Point 5	Point 6	Point 7	Point 8
F_{max}/F_{min}	$F_{d7}/F_{d1}=3.80$	$F_{d6}/F_{d8}=2.77$	$F_{d7}/F_{d8}=4.90$	$F_{d7}/F_{d1}=6.85$
V_{max}/V_{min}	$V_{d6}/V_{d3}=6.86$	$V_{d1}/V_{d3}=5.66$	$V_{d1}/V_{d7}=9.26$	$V_{d6}/V_{d8}=3.66$

7. Conclusion

In this paper, the dual-mode distributed actuation mechanism was proposed for the efficient operation of a finger-type manipulator. Through mathematically deriving fingertip force and velocity, and maximizing them, it was proven that the proposed dual-mode operation provides a mechanical duality which maximizes either a fingertip force or velocity of the manipulator, depending on the task. Numerical results discovered the force and velocity octagons that represent allowable force and velocity along the eight task directions at the given fingertip position in workspace. These information would be vital to optimally design a task-oriented trajectory, thus expending the proposed concept to the real-world robotic manipulators for delicate tasks. Future work will focus on the experimental validation of the proposed dual-mode mechanism.

8. References

[1] J. D. W. Madden, N. A. Vandesteeg, P. A. Anquetil, P. G. A. Madden, A. Takshi, R. Z. Pytel, S. R. Lafontai

- ne, P. A. Wieringa, and I. W. Hunter, Artificial Muscle Technology: Physical Principles and Naval Prospects, *IEEE Journal of Oceanic Engineering*, 29 (3), 706-728, 2004.
- [2] S. Alfayada, F. B. Ouezdoua, F. Namounb, and G. Ghengc, High performance integrated electro-hydraulic actuator for robotics – Part I: Principle, prototype design and first experiments, *Sensors and Actuators A: Physical* 169 (1), 115– 123, 2011.
- [3] S. Seok, A. Wang, D. Otten, and S. Kim, Actuator Design for High Force Proprioceptive Control in Fast Legged Locomotion, in *Proceeding of IEEE/RSJ International Conference on Intelligent Robots and Systems*, 1970-1975, 2012.
- [4] J. Urata, T. Hirose, Y. Namiki, Y. Nakanishi, I. Mizuuchi and M. Inaba, Thermal Control of Electrical Motors for High-Power Humanoid Robots, in *Proceeding of IEEE/RSJ International Conference on Intelligent Robots and Systems*, 2047-2052, 2008.
- [5] T. Takaki and T. Omata, High-performance anthropomorphic robot hand with grasping-force-magnification mechanism, *IEEE/ASME Transactions on Mechatronics*, 16 (3), 583–591, 2011.
- [6] Y. J. Shin, H. J. Lee, K.-S. Kim, and S. Kim, A Robot Finger Design Using a Dual-Mode Twisting Mechanism to Achieve High-Speed Motion and Large Grasping Force, *IEEE Transactions on Robotics*, 28 (6), 1398-1405, 2012.
- [7] Y. J. Shin and K.-S. Kim, Distributed actuation mechanism for a finger-type manipulator: Theory and experiments, *IEEE Transactions on Robotics*, 26 (3), 569–575, 2010.